

## *In situ* ordered polycrystalline FePt $L1_0$ (001) nanostructured films and the effect of CrMn and Zn top layer diffusion

Sangki Jeong,<sup>a)</sup> T. Ohkubo, Anup G. Roy, D. E. Laughlin, and M. E. McHenry  
Data Storage Systems Center, Department of Materials Science and Engineering, Carnegie Mellon University, Pittsburgh, Pennsylvania 15213

The nanostructure and magnetic properties of *in situ* ordered polycrystalline FePt thin films (9 nm) have been studied. Films were deposited with a MgO underlayer onto Si and glass substrates using conventional rf diode sputtering. Perpendicular anisotropy was obtained when the substrate temperature exceeded 490 °C. The maximum order parameter ( $S$ ) was estimated to be  $\sim 0.9$ . The coercivities ( $H_c$ ) ranged from 5 to 12 kOe. Observed high values of the coercive squareness ( $S^*$ ) indicate the existence of exchange coupling. High resolution transmission electron microscopy indicates a defective region which might be associated with defect-related localized incoherent nucleation, thereby inducing low values of  $H_c$ . Zn and CrMn top layers at ambient temperature were deposited after the deposition of FePt films at elevated temperatures. Rapid thermal annealing of these samples at 180–450 °C for 1 min resulted in a decrease of  $S^*$  from 0.8–0.85 to  $\sim 0.5$ –0.6.  
© 2002 American Institute of Physics. [DOI: 10.1063/1.1452249]

FePt thin films have a large magnetocrystalline anisotropy constant that is associated with the tetragonal  $L1_0$  phase. They also have a high saturation magnetization  $M_s$  that makes it possible to decrease the magnetic layer thickness ( $t$ ) below 10 nm to reduce head field gradients<sup>1</sup> while maintaining reasonable  $M_s t$  and perpendicular anisotropy (as well as the thermal stability that arises from the large anisotropy). There have been many reports of the  $L1_0$  thin films.<sup>2–4</sup> Most of the previous results have been based on the growth of perpendicularly oriented  $c$  axes in FePt thin films on single crystal (001) MgO substrates.<sup>3,4</sup> However, there are a few reports on the development of *in situ* ordered polycrystalline FePt (001) films<sup>5</sup> using a MgO underlayer by conventional rf diode sputtering under normal sputtering conditions. But, there are no reports on details of nanostructural observations of this medium, which is necessary for in-depth understanding of the magnetic properties.

Previously, we showed that ambient-temperature deposited, polycrystalline FePt/MgO thin films after rapid thermal annealing (RTA) displayed strong perpendicular anisotropy and small grains.<sup>6</sup> However, a high temperature postannealing process was still required for ordering of the face-centered-cubic (fcc) phase to achieve a reasonably large order parameter to develop high coercivity and perpendicular anisotropy. Moreover, these FePt films showed highly exchange-coupled grains.<sup>6</sup> In this work we have prepared *in situ* ordered polycrystalline FePt thin films with a MgO underlayer using conventional rf diode sputtering. Here we present details of the nanostructure, growth, and magnetic properties as well as the influence of the nanostructure on the magnetic properties. In addition, the possibility of exchange decoupling by diffusion from a nonmagnetic top layer at relatively low temperature (180–450 °C) is discussed.

All films were prepared by rf diode sputtering on 1 in. silicon (100) coupons and 7059 Corning glass substrates.

The sputtering pressure of the Ar gas was in the range of 20–50 mTorr. Films of CrMn (20 nm) and Zn (15 nm) were deposited at ambient temperature on top of a FePt layer. The magnetic properties were measured using vibrating sample magnetometry (VSM) and alternating gradient force magnetometry (AGFM), in fields up to 14–20 kOe. Structural analysis was made by x ray diffractometry (XRD) ( $\text{Cu } K\alpha$ ). Analysis of the microstructure was accomplished by transmission electron microscopy (TEM). The chemical compositions of the films were found to be close to  $\text{Fe}_{51}\text{Pt}_{49}$  by an x-ray fluorescence method. The thickness of the FePt films was fixed at  $\sim 9$  nm. For FePt films, the substrate temperatures were varied to 580 °C. The glass and Si substrates show nearly the same results in the structural and magnetic characterizations.

As shown in Fig. 1, an  $L1_0$  (001) ordered superlattice reflection is clearly observed in the films deposited from 370 °C, indicating the presence of  $L1_0$  (001) grains. However, the (002) reflections overlap the fcc (200) reflections

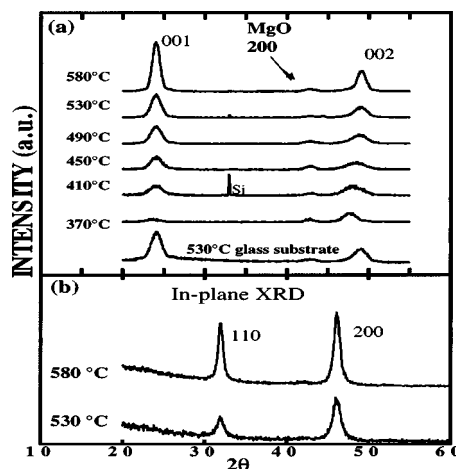


FIG. 1. XRD patterns of FePt 9 nm/MgO 8 nm films at various temperatures.

<sup>a)</sup>Electronic mail: sjeong@andrew.cmu.edu

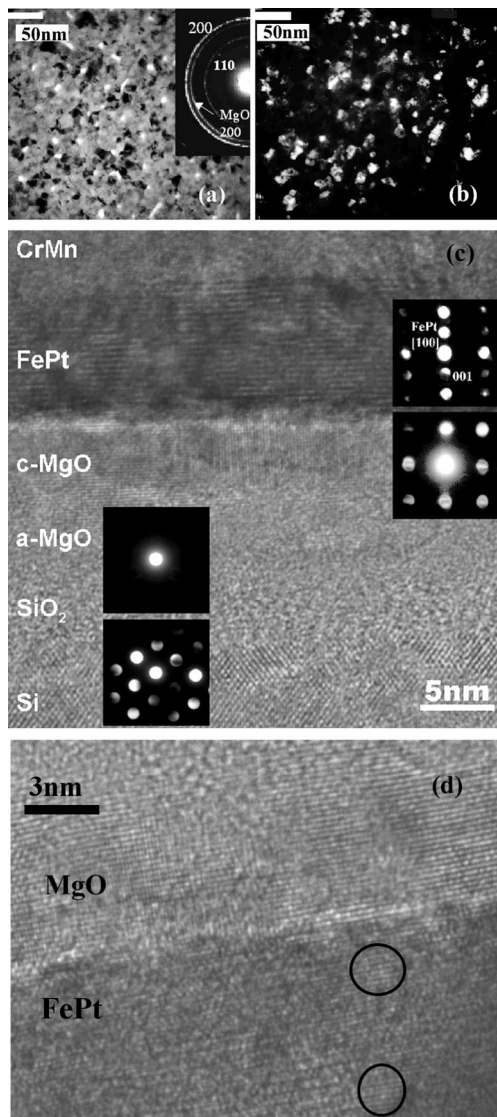


FIG. 2. SAED patterns of the (a) bright and (b) dark fields from TEM (plan view); (c) HRTEM image of a cross section of the films and diffraction patterns by the convergent beam technique; (d) HRTEM image of some inhomogeneous region (cross section). (a), (b) FePt: Deposited at 530 °C; film structure: FePt 9 nm/MgO 8 nm; (c), (d) CrMn/FePt 9 nm/MgO 8 nm.

and cannot be used as unambiguous evidence of the texture. The films deposited at temperature higher than 490 °C exhibit mainly the  $L1_0$  (001) and (002) reflections, indicating the predominance of the  $L1_0$  phase as well as the preferential growth of (001) oriented grains. In-plane XRD ( $\theta/2\theta$  scan) patterns ( $2^\circ$  grazing incidence beam) confirmed the absence of (100) oriented grains and the dominance of perpendicular structural variants. Determining the mechanism for this phenomenon is the subject of ongoing work. The measured integrated intensity ratio of  $I_{001}/I_{002}$  in XRD patterns indicates that the maximum degree of order (long range order parameter,  $S$ ) is close to  $\sim 0.9$  for the films deposited at 580 °C  $\{S^2 = ([I_{001}/I_{002}]_{\text{meas}} / [I_{001}/I_{002}]_{\text{calc}})\}^6$ .

Figure 2 shows TEM nanostructural observations of the FePt films deposited at 530 °C. Selected area electron diffraction (SAED) patterns [Fig. 2(a)] for plan view show a similar intensity profile as the in-plane XRD [Fig. 1(b)], confirming the predominance of (001) oriented grains. However,

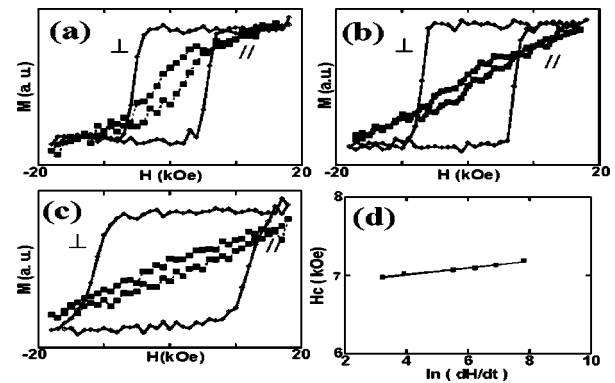


FIG. 3. Hysteresis loops of FePt 9 nm/MgO 8 nm films deposited at (a) 490, (b), and (c) 580 °C. (d) Field sweep rate dependence of  $H_c$  for the film in (b).

it is difficult to identify a small fraction of fcc phase in the XRD and SAED patterns due to the overlap  $L1_0$  (002) reflections. High resolution TEM (HRTEM) along with nanodiffraction by the convergent beam technique has been performed. This confirms the (001) oriented  $c$  axes [Fig. 2(c)] as well as cubic to cubic epitaxial growth. However, as shown in Fig. 2, nano-sized fcc clusters [indicated by a circle in Fig. 2(d)] or less ordered regions can be found in some grains. Assuming the same defocus length and thickness of the specimen in the image, the HRTEM image shows strong intensity every other atomic layer in FePt films due to (001) reflections along the perpendicular direction of the film's plane. Less ordered or fcc regions can give rise to similar intensity in every atomic layer. Since these clusters are smaller than the critical length for exchange coupling,<sup>6,7</sup> they are highly exchange coupled with other areas in a grain. However, This can initiate the magnetization reversal process through defect related incoherent nucleation,<sup>7</sup> resulting in a low value of the nucleation field. As seen in the plan-view TEM image in Fig. 2, most of the grain sizes range from 10 to 15 nm for the films deposited at 530 °C.

The magnetic properties measured at ambient temperature are illustrated in Fig. 3. Perpendicular anisotropy is observed for films grown at 490 °C and above. The coercivities range from  $\sim 5$  to  $\sim 12$  kOe. The coercive squareness ( $S^*$ ) is between  $\sim 0.8$  and 0.85.  $S^*$  reaches around 0.95 in FePt/MgO films fully ordered by the postannealing procedure (RTA), implying that the *in situ* ordered films have more exchange breaking between grains.<sup>6</sup> By applying  $\sim 20$  kOe to the sample deposited at 490 °C, the out-of-plane torque curves showed uniaxial symmetry as well as rotational hysteresis loss which implies that perpendicular anisotropy field  $H_{K_\perp}$  is higher than 20 kOe. This gives rise to the approximate value for the lower bound of  $H_{K_\perp}$ . In taking the demagnetizing energy of a thin film geometry (magnetocrystalline anisotropy constant  $K_u = K_\perp + 2\pi M_s^2$ ,  $M_s \sim 1000$ – $1100$  emu/cc) into account, the measured intrinsic isotropy field  $H_{Ku}$  ( $2K_u/M_s$ ) appears to be larger than  $\sim 33$  kOe for films deposited at 490 °C.

An increase in the coercivity,  $H_c$ , of  $\sim 3\%$  was observed for the sample deposited at 530 °C [Fig. 3(d)], when the sweep rate varied from 2500 to 25 Oe/s. From the field

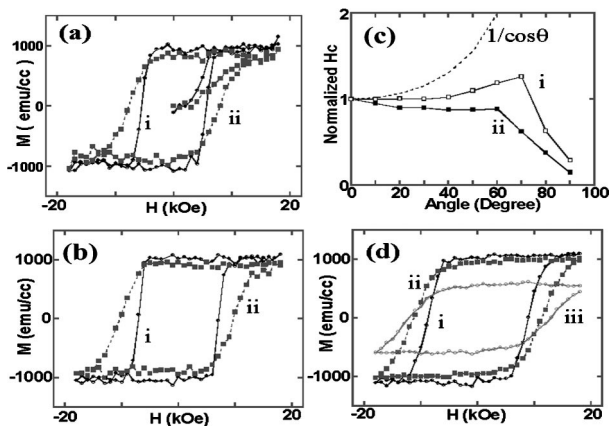


FIG. 4. Hysteresis loops of CrMn 20 nm/FePt 9 nm/MgO 8 nm films (a) before and (b) after RTA at 450 °C for 1 min. The FePt films were deposited at elevated temperatures of (a) 490 and (b) 530 °C whereas the CrMn top layers (20 nm) and MgO layers were prepared at ambient temperature. (c) Angular dependence of  $H_c$  of the sample in (a) before and after RTA: (i) before RTA; (ii) after RTA at 450 °C for 1 min. The angle is defined between the easy axes and the applied field. (d) Hysteresis loops of Zn 15 nm/FePt  $\sim$ 9 nm/MgO  $\sim$ 8 nm films (FePt: deposited at 530 °C; MgO underlayer and Zn top layer: deposited at room temperature) before and after RTA at 180 and 250 °C for 1 min (i) before RTA; (ii) after RTA at 180 °C for 1 min; (iii) after RTA at 250 °C for 1 min.

sweep rate dependence of the coercivity<sup>8,9</sup> we infer that thermal activation during the reversal process is not negligible. Micromagnetic calculations predict  $H_0/H_{Ku}$  [the intrinsic switching field ( $H_0$ )] is larger than 0.3 where each grain is assumed to switch by coherent rotation.<sup>6,10</sup> Therefore, the low value of  $H_c/H_{Ku}$  ( $< \sim 0.1-0.2$ ) might be attributed to reversal processes associated with defect related nucleation as well as thermal activation. We postulate that the nucleation occurs in less ordered regions of the grains as discussed with regard to the nanostructural observations. Research on details of the reversal mechanism will be addressed in future work.

It has been reported that breaking the exchange coupling decreases the medium noise and that there is an optimum state in which the signal-to-noise ratio reaches a maximum.<sup>11</sup> Therefore, it is interesting to investigate the possibility of controlling exchange decoupling by chemical segregation. An earlier report by Zou *et al.*<sup>12</sup> indicated that top or bottom layer diffusion through the grain boundary is one promising method for magnetic isolation. In this study, we have prepared CrMn and Zn top layers at ambient temperature on top of FePt films deposited at elevated temperatures. These samples were postannealed at 450 °C for CrMn/FePt/MgO films and at 180–250 °C for Zn/FePt/MgO films for 1 min using RTA. Zn atoms are expected to be very mobile as is evident from the low melting point of Zn (419 °C). Figures 4(a)–(c) show the hysteresis as well as the angular dependence of  $H_c$  before and after RTA of the samples with a CrMn top layer. There is a dramatic change in  $S^*$ , decreasing from  $\sim 0.85$  to 0.6. The slope at  $H_c$  almost reaches

$\sim 2/4\pi$  which is twice the theoretical value of  $1/4\pi$  for a Stoner–Wohlfarth type particle assembly.  $H_c$  is expected to increase due to the decoupling of grains as well as to the decrease of  $M_s$  ( $\sim 10\%$ ). The angular dependence of the coercivity,  $H_c$ , exhibits a large deviation from domain wall motion mode ( $1/\cos\theta$ ) [Fig. 4 (c)].  $H_c$  decreases as the angle ( $\theta$ ) between the easy axes and the field direction increases for the FePt films (with the CrMn top layer) after being annealed at 450 °C. This implies that the grains are less magnetically coupled and reverse more independently.<sup>13,14</sup> The increase of  $H_c$  is 40%–50%, of which  $\sim 10\%$  can be attributed to a decrease in  $M_s$ , assuming  $H_c \propto 1/M_s$ . The films with a Zn top layer showed a dramatic change in hysteresis even after annealing at 180–250 °C [Fig. 4(d)]. For these, the annealed films could not be saturated in an applied field of 18 kOe. This is evidence of grain isolation caused by the Zn top layer. Since bulk diffusion should be very slow below 500 °C, these phenomena can be attributed to the boundary diffusion<sup>12</sup> of CrMn and Zn, which produces a nonmagnetic layer at the grain boundaries and enhances the decoupling. XRD patterns show the same spectra before and after the annealing process. Preliminary results by chemical analysis in a TEM show a significant amount of Zn diffusion into the FePt layer even at 250 °C. A detailed investigation by chemical analysis is required for a more definitive demonstration of this proposed isolation mechanism. This is the subject of ongoing work.

This research was supported by the Data Storage Systems Center at Carnegie Mellon University under Grant No. ECD-89-07068 from National Science Foundation and in part by the Air Force of Scientific Research, Air Force Material Command, USAF, under Grant No. F49620-96-0454.

- <sup>1</sup>R. Wood, IEEE Trans. Magn. **36**, 36 (2000).
- <sup>2</sup>D. J. Sellmyer, M. Yu, R. A. Thomas, Y. Liu, and R. D. Kirby, Phys. Low-Dimens. Semicond. Struct. **1/2**, 155 (1998).
- <sup>3</sup>D. Weller, A. Moser, L. Folks, M. E. Best, Lee Wen, M. F. Toney, M. Schwickert, J.-U. Thiele, and M. F. Doerner, IEEE Trans. Magn. **36**, 10 (2000).
- <sup>4</sup>R. F. C. Farrow, D. Weller, R. F. Marks, M. F. Toney, S. Hom, G. R. Harp, and A. Cebollada, Appl. Phys. Lett. **69**, 1166 (1996).
- <sup>5</sup>T. Suzuki, N. Honda, and K. Ouchi, J. Magn. Magn. Mater. **193**, 85 (1999).
- <sup>6</sup>S. Jeong, Y. Hsu, D. E. Laughlin, and M. E. McHenry, IEEE Trans. Magn. **36**, 2336 (2000).
- <sup>7</sup>R. Skomski, J. P. Liu, and D. J. Sellmyer, Mater. Res. Soc. Symp. Proc. **577**, 335 (1999).
- <sup>8</sup>P. Bruno, G. Bayreuther, P. Beauvillan, C. Chappert, G. Lugert, D. Renard, J. Renard, and J. Seiden, J. Appl. Phys. **68**, 5759 (1990).
- <sup>9</sup>G. Bottoni, D. Candolfom, and A. Cecchetti, IEEE Trans. Magn. **36**, 2468 (2000).
- <sup>10</sup>S. M. Stinett and W. D. Doyle, IEEE Trans. Magn. **36**, 2456 (2000).
- <sup>11</sup>S. J. Greaves, H. Muraoka, Y. Sugita, and Y. Nakamura, IEEE Trans. Magn. **35**, 3772 (1999).
- <sup>12</sup>J. Zou, B. Bian, D. N. Lambeth, and D. E. Laughlin, 8th MMM-Intermag conference, 2001.
- <sup>13</sup>Y. Chen, Ph.D. dissertation, Carnegie Mellon University, Pittsburgh, PA, 1998.
- <sup>14</sup>R. Ranjan, J. S. Gau, and N. Amin, J. Magn. Magn. Mater. **89**, 38 (1999).